

A versatile method to grow localized arrays of nanowires for highly sensitive capacitive devices

V. A. ANTOHE*, A. RADU^a, S. YUNUS, A. ATTOUT, P. BERTRAND,
M. MÁTÉFI-TEMPFLI, L. PIRAUX, S. MÁTÉFI-TEMPFLI*

Unité de Physico-Chimie et de Physique des Matériaux, U.C.L., Louvain-la-Neuve – 1348, Belgique

^aDepartment of Materials and Electronic & Optoelectronic Devices, U.B., Bucharest-Magurele – 077125, Romania

We propose a new approach to increase the detection efficiency of the capacitive sensing devices, by growing vertically aligned nanowires arrays, localized and confined on small interdigitated electrodes structures. The metallic tracks are made using optical lithography, and the nanowires are realized by electrochemical synthesis in nanoporous materials (i.e. supported alumina templates). By controlling the preparation conditions, both their positions and pitches can be easily tuned, as well as their geometrical design (i.e. diameters between 5 – 350 nm and lengths between 150 nm – 10 μm). Based on these considerations, a capacitive sensor structure with high active surface is sensitized with polyaniline, for pH detection. Reported data show that the sensitivity of the sensor is substantially improved by using nanowires arrays.

(Received September 1, 2008; accepted October 30, 2008)

Keywords: Electrochemical Synthesis, Alumina Templates, Nanowires, Polyaniline, pH Sensors

1. Introduction

Today one of the great challenges in nano-technology is to find reliable techniques for the fabrication of nanometric capacitive sensing devices, with increased active surface, in order to reach high detection sensitivities. Complex fabrication procedures dealing with advanced nanostructuring methods, that allow an easy access and control of the geometrical factors and positioning are currently employed, further targeting large-scale integration. Designing new type of sensors, in which changes in the electrical properties of a functionalized electrode surface are detected, represents a real challenge. Using interdigitated electrodes, the changes can be evaluated by measuring either the electrical capacity or impedance [1-4]. The greatest efforts are related with increasing the active surface area of such electrical transducers, in order to reach higher sensitivities, while keeping dimensions in the nanometer range.

Taking these into account, nanowires or nanotubes are ideal candidates for such devices, due to their easiness of large area production, and low-cost fabrication processes [5]. The fabrication of nanowires (NWs), involves their synthesis within nanoporous templates such as supported alumina (Al_2O_3) membranes. This template, made by electro-chemical oxidation of aluminum has been widely used because it provides a good platform for the development of different nanostructures [6-8]. However, the use of large areas of nanostructures (nanowires), as active parts from electronic devices requires specially designed arrays of NWs with well defined patterns, positions and pitches. Recent work was focused on the fabrication of localized NWs arrays, within alumina membranes by patterning the substrate using an advanced lithographic method [9,10].

Therefore, by combining the powerful tools of the lithographic techniques with the electrochemical template synthesis using alumina membranes we developed a simple approach for the localized growth of the platinum NWs on top of small interdigitated electrode structures (IDES). The process is performed using a supported alumina membrane as a template, fabricated on top of a conductive underlayer that was before patterned by an advanced lithographic method. A subsequent electrochemical deposition inside nanopores allows then the NWs to grow locally, only on the conducting electrodes. Further, growing an additional layer of polyaniline (PANI), sensitive to pH changes, on the surface of Pt nanowires based structures we prepared a capacitive pH sensor with high sensitivity.

The measurements of the frequency response of a parallel LC circuit, containing our sensor, were carried out to demonstrate that a substantial increasing in its sensitivity has been obtained, as a result of the increasing of its active surface, using the PANI covered perpendicular NWs.

2. Experimental

Fig. 1 shows a schematic overview of the fabrication steps. The entire process started with a physical vapor deposition of a conducting underlayer (~ 50 nm) of platinum, on a carefully cleaned SiO_2 (100 nm) / Si substrate. The deposited metallic thin layer plays a double role in the fabrication process. On one hand, it serves as anodization barrier during the further electrochemical oxidation of the aluminum layer, and on the other hand, it acts as contacting electrode during both, oxidation (anodization) and electrochemical

deposition of the NWs. A thin titanium layer (~ 10 nm) was also used, for a better adherence between the conducting underlayer and SiO_2/Si substrate.

For defining the IDE structure, the substrate was patterned using an optical lithography process. The IDE geometry was especially designed for capacitive sensing and for facilitating a good electrical contact for further measurements. Typical dimensions of electrode widths and interspaces vary in the $1 - 2 \mu\text{m}$ ranges. The lithographic process ended with a soft oxygen plasma etching, for a better cleaning of the eventual organic contamination that could occur during the lithography steps.

Further, a thick aluminum layer ($\sim 1 \mu\text{m}$) was sputtered on the top surface of the patterned substrate. This was a critical step in our fabrication process, in the sense that small thicknesses (up to few hundreds of nm) are easy to obtain but thicker ones need special deposition conditions, for avoiding the possible hillocks or pitting defects [11].

The prepared wafer was subsequently used in an electrochemical template synthesis, starting with the anodization of the aluminum layer inside an electrolytic cell. To allow the formation of nonporous alumina (Al_2O_3) membrane, a controlled oxidation of Al, was conducted, where the anode was the sample itself, the cathode was a pure aluminum bar and the electrolyte was a solution of 0.3 M oxalic acid. The oxidation conditions were carefully chosen, for obtaining a uniform and dense nanoporous membrane. The process was performed at 2°C and an anodization voltage of 60 V was applied to obtain the desired spaces between the pores (~ 150 nm). The voltages were applied using a Keithley 2400 controlled by a computer via a GPIB interface. By controlling the current at the end of the anodization process, when no more metallic aluminum remained on the substrate, nanopores down to the interdigitated tracks were obtained. Subsequently the nanopores were enlarged to diameters of ~ 90 nm during a chemical widening process, performed at $\sim 30^\circ\text{C}$ with a phosphoric acid solution of 5 wt%.

Once the pores were properly defined, an electrochemical deposition process was performed in the same electrolytic cell, using a conventional three electrodes potentiostatic method, where the cathode was the sample itself, the anode was a platinum foil and the reference was an Ag/AgCl electrode. A Princeton Applied Research Potentiostat/Galvanostat 263A has been used for the electrochemical deposition of platinum, inside the nanopores of the supported alumina template, by applying a continuous voltage of -0.3 V using a commercial Pt electrolyte of Platinum - OH - Bath (Metakem). The process was performed at $\sim 50^\circ\text{C}$. By controlling the deposition time, the effective length of the NWs growing inside the nanopores can be successfully regulated. Lengths of up to ~ 500 nm were adopted in order to obtain vertically aligned (to the substrate) NWs arrays after the alumina host removal step. This step was performed by a chemical dissolution of the Al_2O_3 membrane, using a 2 M solution of NaOH .

The sample was then carefully cleaned using deionized water.

A second lithography step was performed, by masking the entire surface with a SiN layer to generate opened windows only on top of the IDE areas. In this way, the NWs were further confined to grow only on the active surface of the structures.

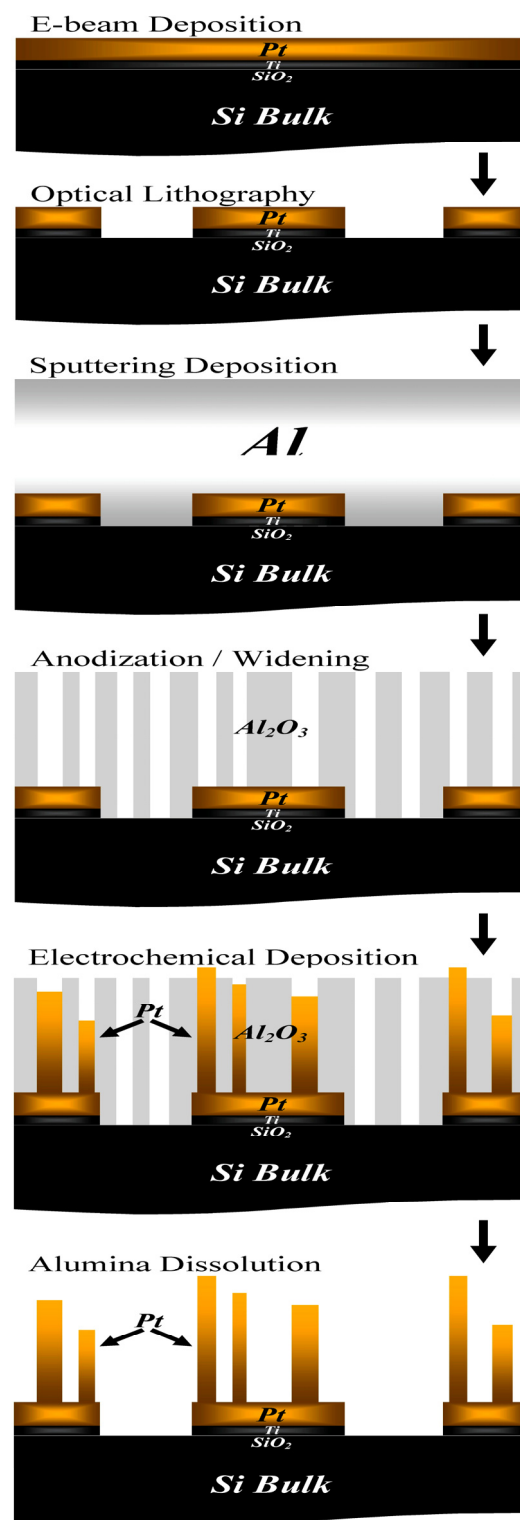


Fig. 1. Schematic representation of the fabrication process for growing and localizing nanowires (NWs) on top of interdigitated electrodes structures (IDEs).

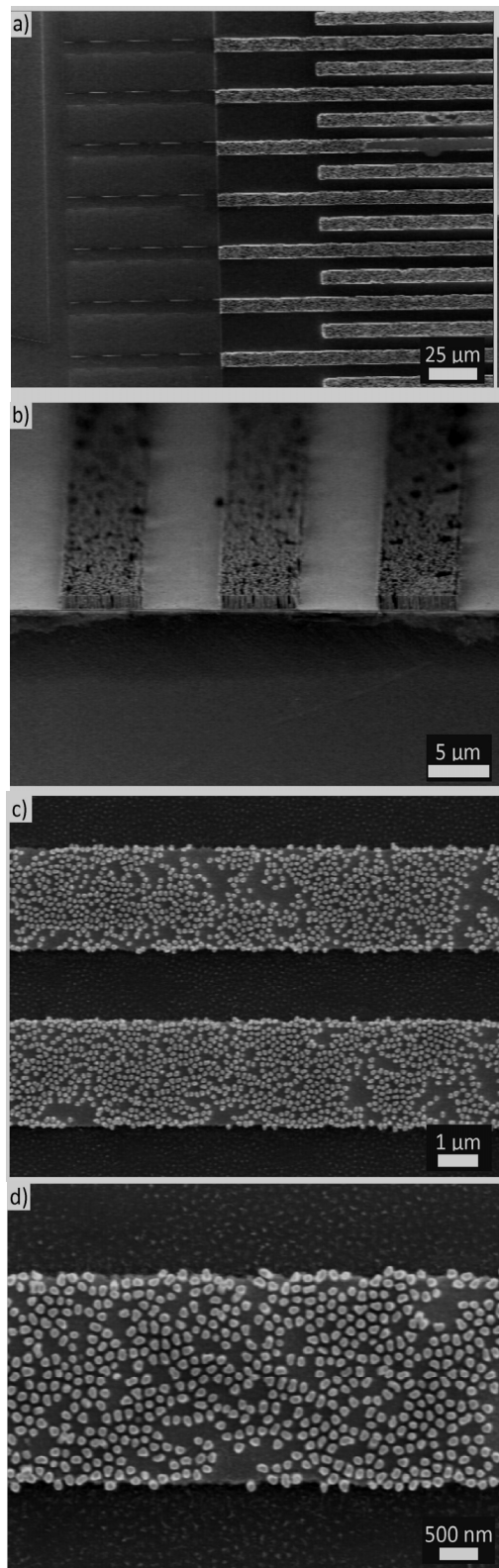


Fig. 2. SEM micrographs of the Pt NWs localized on Pt IDEs. The widths of electrodes and interspaces are in the 1 – 2 μm range. The diameter of the wires is around 90 nm and their length is up to 500 nm. The distance between two adjacent NWs is around 150 nm. The images were taken with increasing magnification from (a) to (d), after the removal of the alumina host. The protection role of the SiN mask against the growth of NWs in the non-interest area can be noticed (a).

Fig. 2 shows the scanning electron microscope (SEM) images (top view and angle view) of the different Pt IDEs with localized Pt NWs, uniformly grown and perpendicularly aligned to the substrate, using the techniques presented above. Such vertically aligned NWs arrays realized on microelectrodes, are very promising for applications where high active surfaces are needed, i.e. capacitive sensors or biosensors.

Therefore, we adopted a simple approach of creating a capacitive pH sensor, by growing an additional layer of polyaniline (PANI) on the Pt NWs based structures, prepared as shown above [12].

The PANI was deposited on top of our structures by an autocatalytic process (the electroless deposition technique), where the Pt NWs and the IDEs serve as catalyst. The deposition conditions and timings were carefully chosen in order to obtain a thin layer of PANI (~ 30 nm) on the entire surface of the Pt structure, keeping a high active surface on our micro-interdigitated area (see figure 3) [13].

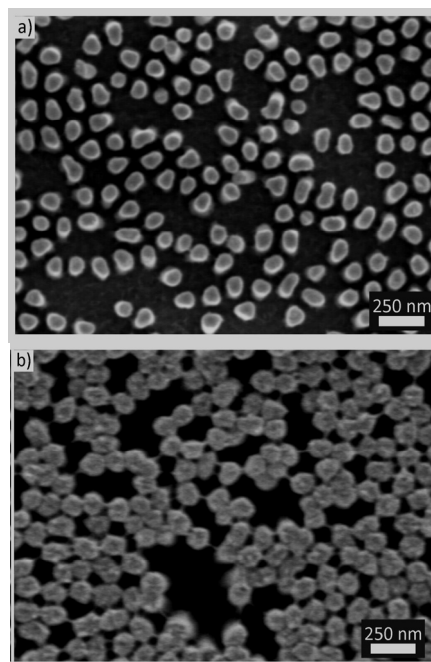


Fig. 3. SEM micrographs of a Pt NWs based structure, before (a) and after (b) PANI deposition. The deposition time of 3 hours, leads to a thickness of ~ 30 nm. The uniformity of the PANI layer on the wires, as well as, the difference in the wire diameters before and after the deposition can be noticed.

PANI, an electro-conductive organic polymer, was chosen as an electrochemical transducer, to sensitize the nanostructured IDE to pH activity. The PANI electrochemical activity is strongly affected by the proton concentration and / or the coupled redox activities [14,15]. These changes could be electrically detected, either by measuring the impedance of the system, or simply by measuring the total capacity of such structure, in different pH conditions.

3. Results and discussion

Impedance measurements were already reported, using small interdigitated structures covered by polyaniline [16,17]. Further, the experiments were focused on measuring the total capacity of such structures, using the simple theory of a parallel LC resonant circuit.

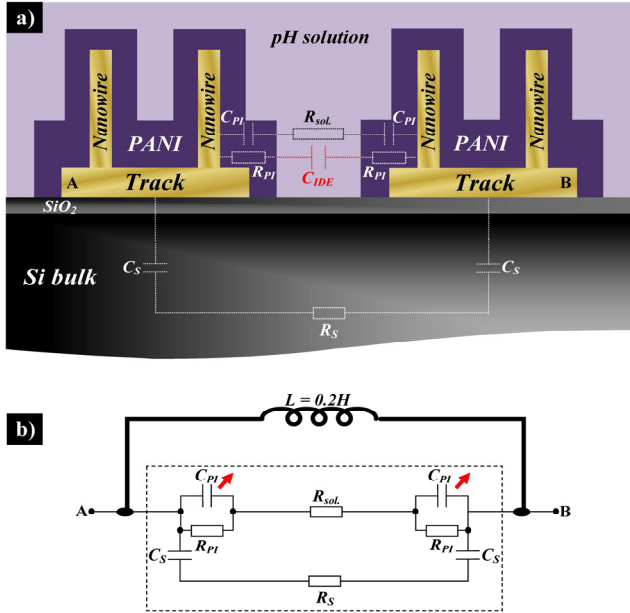


Fig. 4. A transversal sketch of a pH sensor with high active surface (a). The PANI leads to an electrical equivalent circuit (b) used in addition with an external inductance ($L = 0.2 \text{ H}$), for resonance measurements. C_{IDE} is the electrical capacity formed between two consecutive tracks. C_S and R_S are the parasitic capacitive and resistive components respectively, through the Si substrate. C_{PI} and R_{PI} are the complex components of the PANI layer and of the electrical double layer formed on its surface, in the solution. R_{sol} is the resistive component of the pH buffer solution.

The sample was introduced in a resonant circuit by adding a parallel external inductance ($L = 0.2 \text{ H}$). Measuring the frequency response of the resulted system, the total capacity can be calculated using the Thomson formula:

$$f_r = 1/2\pi\sqrt{LC} \quad (3.1)$$

Figure 4a shows a transversal sketch of a pH sensor. Since the PANI/electrolyte interface has a complex electrical behavior, we can consider an electrical equivalent circuit (figure 4b), that was further used as a theoretical model during the measurements.

The frequency sweeping was performed with a 7265 DSP Lock-in Amplifier, controlled by the computer via a GPIB interface. The samples were contacted and manipulated, using a specially designed Printed Circuit Board (PCB). The PANI covered nanostructured IDE

surface was confined in a silicone well, while dropping $100 \mu\text{l}$ of different pH test solutions.

Fig. 5 shows the frequency response, taken on a sample covered by a thin layer of PANI ($\sim 30 \text{ nm}$), in air. It revealed a total capacity of $\sim 500 \text{ pF}$.

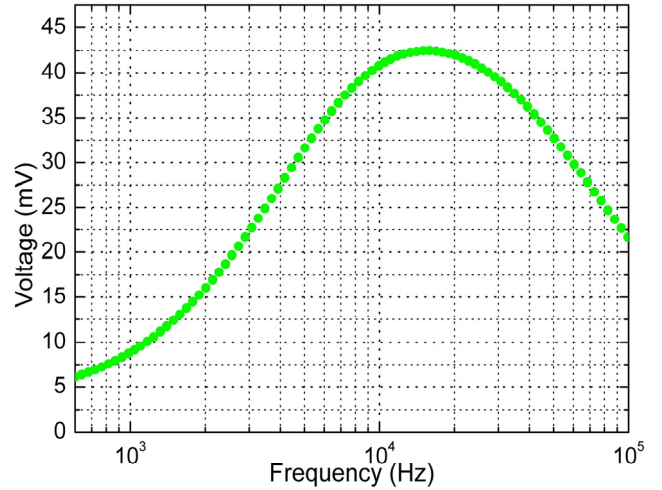


Fig. 5. Frequency response, measured in air. The resonance frequency: $f_{r(\text{air})} = 15.90 \text{ kHz}$ leads to a total capacity: $C_{T(\text{air})} \cong 500 \text{ pF}$.

Fig. 6 depicts the resonance characteristics, of two other samples, one with low active surface (empty IDEs – figure 6a) and one with high active surface (IDEs with vertically aligned Pt NWs – figure 6b), both covered by $\sim 30 \text{ nm}$ of PANI. The measurements were performed in two pH environments (pH 5 – empty blue circles and pH 7 – solid red circles).

Based on the measurements made in open air (figure 5), we can conclude that the electrical capacity formed between two adjacent tracks (C_{IDE}), depicted in figure 4, is really smaller in respect to the other capacities involved in the system (C_S or C_{PI}). The results can be explained by the high distance generated between the metallic pads. This led to a small total capacity of the system, estimated at $\sim 500 \text{ pF}$ (see table 1).

The capacitive components of the PANI/electrolyte interface layer (C_{PI}) were definitely higher due to both, the increased active surface by growing NWs and the presence of the electrical double layer appearing on the surface of the PANI layer when the structure is immersed in the analyzed environment. Using a well conductive solution as environment (a pH buffer solution with good conductivity of $\sim 11 \text{ mS/cm}$), a short circuit of the C_{IDE} is generated. A closer look to figure 6, revealed the fact that the total capacity of the system already jumped in the nF range, meaning, a considerable improvement in respect to the air measurement. Taking this into account, changes in the total capacity of the system were now easily to be detected.

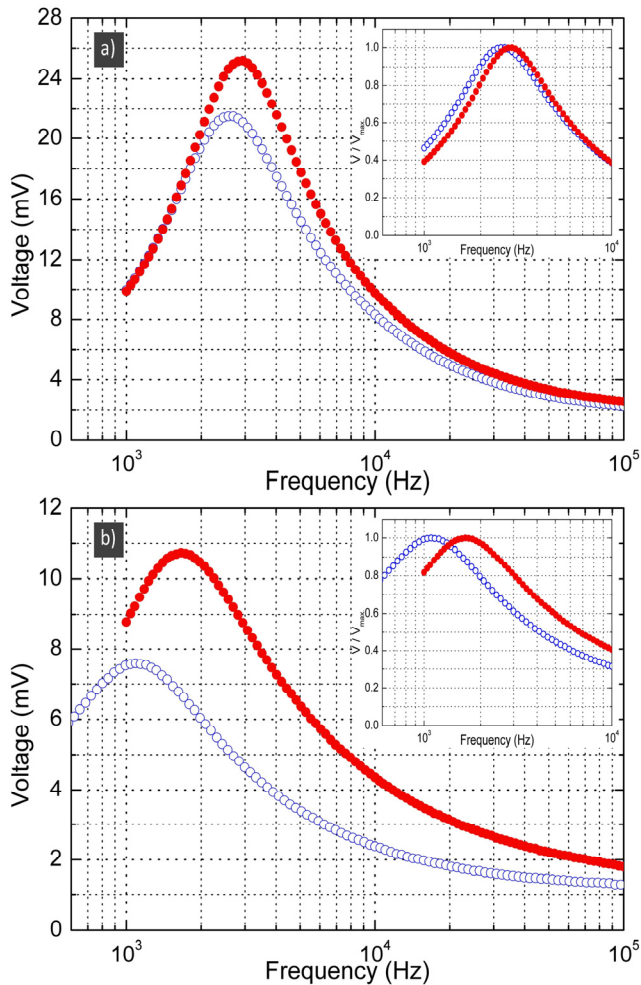


Fig. 6(a). Frequency response for a sample with low active surface, in two pH conditions (pH 7 – solid red circles, pH 5 – empty blue circles). Inset – the corresponding normalized and magnified plots: $f_{r(pH7)} = 2.94$ kHz ($C_{T(pH7)} = 14.65$ nF) and $f_{r(pH5)} = 2.57$ kHz ($C_{T(pH5)} = 19.17$ nF). (b) Frequency response for a sample with high active surface, in two pH conditions (pH 7 – solid red circles, pH 5 – empty blue circles). Inset – the corresponding normalized and magnified plots: $f_{r(pH7)} = 1.66$ kHz ($C_{T(pH7)} = 45.96$ nF) and $f_{r(pH5)} = 1.09$ kHz ($C_{T(pH5)} = 106.60$ nF).

The next step was focused on the sensitivity comparison between a conventional capacitive pH sensor with low IDEs surface and a pH sensor with Pt NWs perpendicularly confined on top of its active surface (figure 6), both measured in the same conditions, using different pH solutions.

The shifts in the resonance frequency (between pH 7 and pH 5) were detected in both cases (with and without NWs grown on IDEs PANI covered samples), as the C_{PI} parts become comparable with the other capacities of the system (C_{IDE} being neglected). Moreover, increasing the active surface of the pH sensor, led to an even higher increase of these components, reflected by the grate shift in the resonance frequency (figure 6b).

Summarizing, all these results demonstrate a superior relative change in the total capacity (between the two pH

solutions) of the sensor of at least 132 %, in the favor of the Pt NWs based device (see table 1).

Taking into account, the resistive components of the PANI layer (R_{PI}), a decrease of the quality factor (Q), with increasing the active surface, can be observed as well. This could be explained, by the decrease of the electrical resistance with the increase of the active surface, in the case of the PANI resistive components (R_{PI} – see figure 4). Moreover, large changes of the quality factor were detected in solutions with different pH values. This phenomenon is explained in terms of the PANI behavior, which became more conductive while moving from basic to acidic environments, by changing its oxidation states [18,19].

Table 1. Comparison between the relative capacitive changes of two samples with and without NWs, respectively. The remarkable increase of the sensitivity in the favor of the NWs based sensor can be noticed.

Analyzing Environment	Total Capacity (nF)	
	pH Sensor without nanowires	pH Sensor with nanowires
In Air	0.500	
pH 5	19.17	106.6
pH 7	14.65	45.96
Capacitive Relative Change	~ 31 %	~ 132 %

A good thing is that the changes in the resistive components of the PANI did not influence the resonance peak, giving just a different band selectivity behavior for the frequency response. Though the quality factor can be improved by controlling the PANI thickness, or changing the external inductance to a lower value, optimal conditions should be found, as the resonance can be completely hidden, if R_{PI} become too small. To keep the highest active surface of the sensor, changes in the PANI thickness are possible in the limit of the geometrical factors of the NWs. Adjustment of the external inductance is also limited to the area where the lock-in amplifier has a linear frequency response.

4. Conclusions

The present paper describes a versatile method for the fabrication of arrays of vertically aligned nanowires on top of interdigitated micro-scale metallic electrodes. Better performances of the new designed complex nano – architecture devices were realized by combining the lithographic techniques with electrochemical synthesis using supported nanoporous alumina templates.

The method allows an easy tuning of the geometrical parameters of the nanostructures and it facilitates an easy

positioning and pitching of the brush structure. The substrate could be patterned in different ways due to the powerful lithographic techniques (micro or nano patterns using optical or e-beam lithography), so that the NWs will grow localized only on the metallic layouts.

The electrochemical synthesis within supported alumina templates creates an easy environment for adjusting the geometrical factors of the NWs. The *Al* layer, which was sputtered in the beginning, dictates the maximal length of the wires, while the electro-deposition timing determines their effective lengths. Also, the widening process of the pores defines the diameters of the pores, simply, by controlling the enlargement time and acid solution temperature. The anodization voltage ensures the distance between the pores and further, the final interspaces between the wires. All these demonstrate the versatility of the proposed preparing method.

Moreover, the fabrication method described here, opens the way for complex devices and circuit fabrication, exploiting the particular properties of the nanowires and nanostructures. Not in the least, due to its flexibility, it facilitates the large-scale integration, being easy to create large areas of localized NWs, for applications requiring large active surfaces for reaching high sensitivities, such as the sensors or biosensors.

The shifts in the resonance frequency of the LC circuit, including our prepared sensors, generated by two different pH solutions, demonstrate that a substantial increase in the sensitivity of a capacitive pH sensor has been possible, due to increasing of its active surface, by using perpendicular NWs, fabricated with our techniques described above.

Work is now in progress to go further for generating specific nanostructures, so that, they can be used both in fundamental studies, as well as in devices fabrication, for improving their performances.

Acknowledgement

We kindly thank to Augustin DUȚU, Dana ȘERBAN and Alexandru VLAD for providing us the *Pt* micro-electrode substrates. We gratefully acknowledge financial support for this study from the Government of the Walloon Region (NANOTIC project).

References

- [1] C. Berggren, B. Bjarnason, G. Johansson, *Electroanalysis*, **13**(3), 173-180 (2001).
- [2] Yi Cui, Q. Wei, H. Park, C. M. Lieber, *Science*, **293** (5533), p. 1289-1292 (2001).
- [3] B. Yang, B. Aksak, Q. Lin, M. Sitti, *Sensors and Actuators B*, **114** (1), p. 254-262 (2006).

- [4] A. Simonis, H. Lüth, J. Wang, M. J. Schöning, *Sensors*, **3**, p. 330-339 (2003).
- [5] M. S. Dresselhaus, Y. M. Lin, O. Rabin, A. Jorio, A. G. Souza Filho, M. A. Pimenta, R. Saito, Ge. G. Samsonidze, G. Dresselhaus, *Materials Science and Engineering C*, **23**, 129 (2003).
- [6] L. Piraux, K. Renard, R. Guillemet, S. Mátéfi-Tempfli, M. Mátéfi-Tempfli, V. A. Antohe, S. Fusil, K. Bouzehouane, V. Cros, *Nano Letters*, **7**(9), 2563 (2007).
- [7] W. Lee, R. Ji, U. Gösele, K. Nielsch, *Nature Materials*, **5**, 741 (2006).
- [8] J. C. Hulteen, C. R. Martin, *J. Mater. Chem.* **7**(7), 1075 (1997).
- [9] S. Mátéfi-Tempfli, M. Mátéfi-Tempfli, A. Vlad, V. A. Antohe, L. Piraux, *J. Mater. Sci.: Mater. Electron.*, DOI: 10.1007/s10854-008-9568-6;
- [10] A. Vlad, M. Mátéfi-Tempfli, V. A. Antohe, S. Faniel, N. Reckinger, B. Olbrechts, A. Crahay, V. Bayot, L. Piraux, S. Melinte, S. Mátéfi-Tempfli, *Small*, **4**(5), 557 (2008).
- [11] S. Mátéfi-Tempfli, *Leading Edge Nanotechnology Research Developments: Nanostructures Grown Via Electrochemical Template Methods*, **Ch. 10**, p. 235-256, Nova Science Publishers, Editor: Sabatini, D. M., New York (2008);
- [12] H. Sangodkar, S. Sukeerthi, R.S. Srinivasa, R. Lal, A. Q. Contractor, *Anal. Chem.*, **68**, 779 (1996).
- [13] A. Attout, S. Yunus, P. Bertrand, *Surf. Interface Anal.*, **40**, 657 (2008).
- [14] N. Gospodinova, L. Terlemezyan, *Prog. Polym. Sci.*, **23**, 1443 (1998).
- [15] G. Bidan, E. M. Genies, J. F. Penneau, *J. Electroanal. Chem.*, **271**, 59 (1989).
- [16] H. Okamoto, Y. Ando, T. Kotaka, *Syntetic Metals*, **96**, 7 (1998).
- [17] M. Irimia-Vladu, J. W. Fergus, *Syntetic Metals*, DOI: 10.1016/j.synthmet.2006.11.004;
- [18] A. G. Macdiarmid, J. C. Chiang, A. F. Richter, *Syntetic Metals*, **18**, 285 (1987).
- [19] J. Chiang, A. G. Macdiarmid, *Syntetic Metals*, **13**, 193 (1986).

*Corresponding author: vlad.antohe@uclouvain.be ,
matefi@uclouvain.be